

RESEARCH ARTICLE

The *N*-terminal tail of the glycine transporter: role in transporter phosphorylation.

Authors

Gentil, Luciana Giroto[‡]; Castrejon-Tellez, Vicente[§]; Pando, Miryam[‡]; Barrera, Susana[‡]; Pérez-León, Jorge Alberto[‡]; Varela-Ramirez, Armando[‡]; Shpak, Max* and Miranda, Manuel[‡].

Affiliations

[‡]Department of Biological Sciences and Border Biomedical Research Center, University of Texas at El Paso, El Paso, TX, 79968, USA.

[§]Department of Physiology, Instituto Nacional de Cardiología “Ignacio Chávez”, México, D.F. México.

*Center for Systems and Synthetic Biology, University of Texas, Austin, TX 78712, USA

Correspondence:

Manuel Miranda

Department of Biological Sciences and Border Biomedical Research Center, University of Texas at El Paso, 2.166 Biosciences Research Building, 500 West University Avenue, El Paso, Texas 79968, Telephone: (915) 747-6645; FAX: (915) 747-5808; E-mail:

mmiranda3@utep.edu

Abbreviations: PMA, 4- α -phorbol 12-myristate 13-acetate (phorbol ester); PKC, protein kinase C; GlyT, glycine transporter; PAE, Porcine Aortic Endothelial cells; DAT, dopamine transporter; NET, norepinephrine transporter; SERT, serotonin transporter; BIM, bisindolylmaleimide I.

Abstract

In the vertebrate nervous system, glycinergic neurotransmission is tightly regulated by the action of the glycine transporters 1 and 2 (GlyT1 and GlyT2). Unlike GlyT1, the GlyT2 is characterized by the presence of a cytosolic 201 amino acids *N*-terminal tail of unknown function. In the present study we stably expressed a set of GlyT2 *N*-terminal deletion mutants and characterized the effect on uptake, trafficking and PKC-dependent post-translational modifications. The deletion of the first 43, 109 or 157 amino acids did not affect the trafficking and maturation of GlyT2. Similarly, a chimeric protein replacing GlyT2 *N*-terminus by the corresponding tail of GlyT1b or deletion of the entire *N*-terminus domain (Δ 201), were able to reach the plasma membrane but showed faster turnover compared to the wild-type. All of these mutant proteins appeared as a mature, glycosylated transporter and a lower protein band corresponding to the non-glycosylated transporter. Interestingly, glycine uptake and PKC-mediated endocytosis and further reduction of transport were not affected by the deletions of 43–157 amino acids. Moreover, the analysis of PKC-dependent post-translational modifications for the mutants demonstrated that GlyT2 transporter ubiquitination was not affected; however, PKC-dependent transporter phosphorylation was completely abolished in the deletions of 157 and 201 amino acids. Altogether, these results suggest that the GlyT2 *N*-terminus does not directly participate in the modulation of transport properties but it could be relevant for scaffold formation and retention at active zones or communication to an intracellular signaling pathway.

Keywords: phosphorylation, ubiquitination, glycine, transporter, PKC

1. INTRODUCTION

The amino acid glycine functions as a major inhibitory neurotransmitter, mainly expressed in the spinal cord and brain stem, where it regulates a variety of motor and sensory functions such as vision, breathing, audition and pain perception (1). Upon neuronal depolarization, glycine is released into the synaptic cleft where binding to postsynaptic receptors (GlyR) induces channel opening and chloride influx, resulting in hyperpolarization of the postsynaptic neuron, thereby preventing the generation of action potentials. The clearance of neurotransmitter from the cleft and termination of inhibitory neurotransmission is achieved by rapid reuptake of glycine back into the presynaptic neuron through the action of the two glycine transporters (GlyTs) GlyT1 and GlyT2, encoded by two different genes (2,3). The GlyTs are Na⁺, Cl⁻-dependent transporters that belong to the SLC6 family, members of which are characterized by shared topology including 12 membrane-spanning domains, a large extracellular loop between spanning domains 3 and 4 containing glycosylation sites and intracellular N- and C-terminal tails (4). Although the GlyTs share 50 % amino acid sequence identity, their main structural differences are highlighted by the length of the N-terminus and the amino acid sequence of both N- and C-terminal tails, with GlyT2 having an extended N-terminus (~200 amino acids in rat, mouse and human) of unknown function. In contrast, the length of the N-terminal tail of GlyT1 and other SLC6 family members is much shorter: 30-91 amino acids for the different isoforms (5,6). Despite the essential role of GlyT2 for animal survival and the extensive structural homology between GlyT2 and GlyT1, very little efforts have been dedicated to understanding the structure and function relationships of GlyT2 N-terminal domain (7).

The distribution of GlyT1 is widespread and abundant in caudal regions of the CNS, in addition to several areas of the diencephalon and the retina; and is localized in astrocytes and neurons (8-11). On the other hand, GlyT2 is found only in the pre-synaptic nerve terminals of glycinergic neurons, highly abundant in neurons from the brain stem, cerebellum and spinal cord (9). Both GlyT1 and GlyT2 play an important role in the duration of glycinergic neurotransmission and GlyT2 is required for the reuptake of glycine into the presynaptic terminal and its subsequent loading into synaptic vesicles by the vesicular inhibitory amino acid transporter (VIAAT) (12). The important role of GlyT2 in the efficacy of glycinergic neurotransmission is highlighted by the fact that point and frameshift mutations mapping to the GlyT2 gene are associated with hyperekplexia. Hyperekplexia, also known as startle disease, is a neuromotor disorder characterized by exaggerated startle responses, irregular breathing, impaired motor coordination, tremors, and muscular spasticity disease (13). Interestingly, these mutations mapped to different regions of the protein including the N- and C-terminal tails, different membrane spanning segments, and both intracellular and extracellular loops (13,14). Similarly, mutations in different regions of the pentameric glycine receptor, GlyR α 1 or GlyR β subunits resulted in hyperekplexia, showing a tight control between pre- and postsynaptic glycinergic neurotransmission (reviewed in (15)).

The efficiency of glycine re-uptake into presynaptic neurons is controlled by the total levels of cell surface glycine transporters, whose levels are strongly influenced by the delivery of newly synthesized transporter to the plasma membrane and by the rates of endocytosis and recycling. For many transporters in the SLC6 family, these trafficking processes are regulated by post-translational modifications

and/or interaction of amino acid residues lying along the cytosolic *N*- and *C*-terminal tails of these carriers (16-18). Abundant experimental evidence demonstrates the role of PKC (*Protein Kinase C*) in regulating trafficking and activity of GlyTs. Specifically, PKC activation by phorbol ester results in a reduction of transport capacity, accelerated transporter endocytosis and enhanced ubiquitination and phosphorylation of amino acid residues lying within the *N*- and/or *C*-terminal tails (18-21). Interestingly, it has been suggested for GlyT2 that acidic substitutions at the conserved residues Thr-419, Ser-420 and Lys-422 located in the second intracellular loop abolished PKC-dependent internalization and inhibition of transporter activity (22). On the other hand, the *C*-terminus of GlyT2 contains a type III PDZ binding site that interacts with PDZ domain containing protein Syntenin-1 to assist in the trafficking of GlyT2 to synaptic sites in cultured neurons (23,24). The GlyT2-Syntaxin 1 interaction has been suggested to increase trafficking of the GlyT2 transporter to the plasma membrane in a calcium dependent manner. Although the GlyT2-Syntaxin binding site was not studied, syntaxin interacts with the *N*-terminus of the serotonin and dopamine transporters (25-28). Moreover, the GlyT2 *N*-terminal domain (residues 135-184) serves as a binding site for the phosphoprotein Ulip6, a member of the collapsin response mediator protein family, however the precise function regulated by this interaction has not been described (29,30).

As mentioned above, the GlyT2 *N*-terminus represents the largest tail of the SLC6 family in vertebrates and its function has not been analyzed. Given the relevance of

this domain in protein-protein interactions and a potential role in regulating several aspects of GlyT2 function or trafficking, we analyzed the function of this unique *N*-terminal domain by characterizing the effects of a series of deletion mutants on the PKC-dependent trafficking, post-translational modification and glycine uptake. The results presented here suggest that the *N*-terminus domain provides stability at the plasma membrane and reveal the presence of several phosphorylation sites that may be important for protein-protein interaction and localization at the plasma membrane.

2. EXPERIMENTAL PROCEDURES

2.1 Plasmid Constructs

The cDNA encoding the human GlyT2 (SLC6A5) was cloned into the pcDNA3.1 (+) vector (Invitrogen) and tagged with a Flag and 10X His epitope tags (FH) at the *N*-terminus, resulting in the final construct FH-GlyT2 (Wild-type). Sequential deletions of the GlyT2 *N*-terminus were obtained by PCR and subcloned into the FH-GlyT2 plasmid. To generate the *N*-terminus deletions: GlyT2- Δ 43, GlyT2- Δ 109, GlyT2- Δ 157 and GlyT2- Δ 201, the forward primers D43-F, D109-F, D157-F and D201-F were used for PCR in combination with GlyT2-R reverse primer (Table 1). In addition, a chimeric transporter (1b Δ T2) resulting from the exchange of the *N*-terminus of GlyT2 by the corresponding GlyT1b *N*-terminus (37 amino acids) was generated using the technique of splicing by overlap extension (SOE by PCR) (31). The resulting PCR products were digested and ligated into the pcDNA3.1 (+) vector. All final constructs were sequenced by automated DNA sequencing prior to transfection.

Table 1: Primer sequence for deletion mutants

Name	Sequence
D43-F	5' TTT <u>GGT ACC</u> ATG GAT TGC GCC GCC CCG CCG CCG CCA CGT 3'
D109-F	5' AAA <u>GGT ACC</u> ATG GAT TGC GGG AGC TCC GGG CCC GGC AAC 3'
D157-F	5' AAA TTT <u>GGT ACC</u> ATG GAT TGC AGC ACCGTG GTG CTG GGC ACG 3'
D201-F	5' AAA <u>GGT ACC</u> ATG GAT TGC CTG TCC ATG GTG GGG TAC GCA 3'
GlyT1-F	5' AAA <u>GGT ACC</u> ATG GCC GCG GCT CAT GGAC 3'
SOE-1/2-F	5' TGG GGC AAC AAA CTG GAC TTC ATC CTG TCC ATG 3'
SOE-2/1-R	5' GTC CAG TTT GTT GCC CCA GTT GCC CCG 3'
GlyT2-R	5' CCC <u>GAA TTC</u> CTA GCA GCA CTG AGT GCC CAG 3'

Underlined sequence indicates the KpnI and EcoRI restriction sites. Bold nucleotides highlight the complementary regions for SOE-PCR

2.2 Cell Culture and Transfection

Porcine aortic endothelial (PAE) cells were grown at 37 °C and 5% CO₂ in F12 medium containing 10% fetal bovine serum and antibiotics. Cells were grown to 50–80% confluence and transfected with plasmids using Effectene transfection reagent following manufacturer recommendations (Qiagen, Hilden, Germany). PAE cells stably expressing wild-type or mutant versions of GlyT2 were selected in the presence of 400 µg/ml of geneticin (G-418).

2.3 Protein purification, western blotting and metabolic labeling

For protein purification, PAE cells stably expressing wild-type GlyT2 or mutants were plated on 35 mm dishes, grown to 100% confluence and treated with vehicle (DMSO) or 1 µM phorbol 12-myristate-13-acetate (PMA) in DMSO for 30 min at 37 °C. After incubation, the cells were placed on ice and washed three times with Ca²⁺- and Mg²⁺-free cold phosphate-buffered saline (CMF-PBS), and the proteins solubilized in lysis buffer (25 mM HEPES, pH 7.6, 10% glycerol, 100 mM NaCl, 10 mM sodium fluoride, 1 mM phenylmethylsulfonyl fluoride, 10 µg/ml leupeptin, 10 µg/ml aprotinin, 1% Triton X-100, 10 mM *N*-ethylmaleimide, 15 mM imidazole) and nutated for 10 min at 4 °C. The resulting lysate was centrifuged at 20,000 x g for 15

min to remove insoluble material. After centrifugation, the cleared lysate was incubated with Ni-NTA agarose beads (Qiagen, Hilden, Germany) for 1 h at 4 °C on a shaker, as previously described (18). Following incubation, the beads were washed five times with lysis buffer and GlyT2 transporter eluted with 250 mM imidazole in lysis buffer. The purified proteins were subjected to 8% SDS-PAGE and western blotting with anti-FLAG M2 (Sigma-Aldrich, St. Louis MO.) or anti-ubiquitin (Santa Cruz Biotechnology, CA.), or anti-C-terminus GlyT2 antibodies (EMD Millipore, Billerica MA.), followed in each case by secondary antibodies conjugated to horseradish peroxidase (Promega, Madison, WI). The protein bands visualization was carried out by using SuperSignal West Pico Chemiluminescent Substrate and by exposure to x-ray films (Thermo Fisher Scientific, Rockford, IL).

For metabolic labeling, confluent stably transfected PAE cells expressing GlyT2 or deletion mutants were incubated in phosphate-free DMEM supplemented with 5% dialyzed-FBS for 8 h following the addition of 100-125 µCi of ³²P-orthophosphoric acid/ml. After 2 h incubation, GlyT2 transporter phosphorylation was stimulated by 1 µM PMA for 60 min or inhibited with 1 µM of

bisindolylmaleimide I (BIM) for 30 min before addition of PMA. As a negative control, parental cells transfected with pCDNA3.1 were incubated with PMA or DMSO. After incubation, cells were washed with PBS and solubilized, as described above, in lysis buffer containing phosphatase inhibitor cocktail and 1 mM sodium orthovanadate. Radiolabeled GlyT2 was purified as described above and subjected to 8 % SDS-PAGE, autoradiography and western blotting labeled with C-terminus GlyT2 antibodies as described above. Western blot band signal intensities were quantitated with ImageJ software (NIH).

2.4 Immunofluorescence Staining

The cells were grown on glass coverslips and treated with 0.1% v/v DMSO or 1 μ M PMA for 30 min at 37 °C. After treatment, the cells were washed with calcium-magnesium free (CMF)-PBS, fixed with freshly prepared 4% paraformaldehyde in CMF-PBS for 15 min, and mildly permeabilized with CMF-PBS containing 0.1% Triton X-100 and 0.5% bovine serum albumin (BSA). The cells were then incubated in CMF-PBS containing 0.5% BSA with primary guinea pig anti-GlyT2 directed against the C-terminus (EMD Millipore, Billerica, MA) or anti-Endosomal Antigen 1, EEA1 (BD Bioscience, San Jose, CA) antibodies for 1 h. After three washes with PBS-BSA, the cells were incubated for 1 h with the corresponding secondary antibodies conjugated with either CY3 or Alexa-488, respectively (Jackson ImmunoResearch Laboratories Inc., West Grove, PA). Cell nuclei were stained with 10 μ g/ml DAPI (Invitrogen, Carlsbad, CA). After staining, the coverslips were mounted in Mowiol reagent. Image acquisition and analysis were performed by using a Zeiss inverted fluorescence Axio Observer Z1 microscope and processed with AxioVision software 7.1 (Carl Zeiss, New York, NY).

The final arrangement of images was performed with Adobe Photoshop software.

2.5 Glycine uptake

The PAE cells expressing wild-type GlyT2 or mutants were grown in 24-well plates to 90-100% confluence and treated with 0.1% DMSO or 1 μ M PMA for 30 min at 37 °C. After treatment, cells were washed three times with reaction buffer at 37 °C (10 mM HEPES-Tris, pH 7.4, 150 mM NaCl, 1 mM CaCl₂, 5 mM KCl and 1 mM MgSO₄) followed by incubation for 10 min in 250 μ l of reaction buffer containing 10 mM glucose, varying concentrations of cold glycine (0.025-1mM) and 4 μ Ci of [³H]-glycine/ml, at 37 °C. The reaction was stopped by removing the medium and washing twice with reaction buffer at 4 °C, followed by lysis in 250 μ l 0.2 N NaOH. Glycine uptake was determined by scintillation spectroscopy and specific activity defined as the difference between GlyT2-mediated glycine uptake and unspecific glycine uptake measured simultaneously from parental cells transfected with pCDNA3.1. Protein concentration was determined by the Bradford method (32), with bovine serum albumin as standard.

2.6 Statistical analysis

Experiments were performed at least in triplicate and are depicted as the average with their corresponding standard deviations or standard errors. The statistical significance among two experimental samples was accomplished by using one-way ANOVA. To determine whether comparisons of two independent samples have statistical significance, a *p* value of <0.05 was considered significant.

3. RESULTS

3.1 Secondary structure and sequence analysis of GlyT2 *N*-terminal domain

Several membrane proteins use the *N*- and/or *C*-terminal tails as regulatory domains to control function or trafficking. For neurotransmitter transporters, post-translational modifications have been suggested to play a role in modulating substrate recognition, uptake rate and trafficking mechanisms (16). In addition, the presence of several consensus sites for phosphorylation by protein kinases and protein binding sites such as WW or PDZ binding sites allow these transporters the connection to signaling molecules and to an intracellular signaling pathway (33-36). Unlike other members of the SLC6 family, the mammalian GlyT2 (SLC6A5) contains a long *N*-terminus that is composed of ~200 amino acids of unknown function. To get structural information of this domain, the primary amino acid sequence of the *N*-terminus was subjected to prediction of secondary structure with different algorithms. Interestingly, PSIPRED, PHD, GOR, NPSA and Porter among many other algorithms predict the presence of three short α -helices followed by three short 5-6 amino acids β -strands whereas the majority of the sequence is predicted to contain coil regions, suggesting a disordered tail (Fig 1A). It is worth mentioning that this domain is rich in proline residues, probably contributing to this disordered structure. As depicted in the *N*-terminal amino acid sequence of the human

GlyT2 of Fig 1A, proline residues are spread throughout the tail, including stretches of 3-4 consecutive prolines. Given the frequency of prolines and the length of the *N*-terminus, we performed a bioinformatics analysis using the Eukaryotic Linear Motifs (ELM, <http://elm.eu.org>) database to look for linear motifs that could represent binding sites for interacting proteins (37). As shown in Figure 1A and Table 2, four predicted non-canonical class 1 SH3 binding sites were identified in the first half of the *N*-terminus. These four regions correspond to two overlapping proline-rich regions (see solid bars in Fig 1A) that fulfill the requirement for a class I XXXPXXP motif (35,38). Interestingly, multiple motifs for proline-directed kinases and WW domain containing proteins that recognize phosphorylated serine/threonine-proline sites were found throughout the entire *N*-terminus, suggesting a possible role of these motifs in directing transporter phosphorylation and possibly connecting the transporter to an intracellular network of interacting proteins. In support of this hypothesis, clear experimental evidence described for SLC6 family members demonstrate that direct and indirect activation of PKC results in transporter phosphorylation and ubiquitination followed by endocytosis (16,39,40). Altogether, this analysis points to the GlyT2 *N*-terminus as a potential platform for protein-protein interaction and complex formation that may trigger post-translational modifications to regulate different transporter properties including localization and trafficking.

Table 2: Prediction of motifs along the GlyT2 *N*-terminus

Domain	Motif or sequence	Domain	Motif or sequence
SH3 non-canonical class	XXXPXXP	WW class III	XPPRX
Proline-directed kinase	23-QGHPDGP-29	WW class IV	47-PPPRV-51
	26-PDGPCAP-32		XXX[S/T]PX
	43-AAAPPPP-49		13-PANSPE-18
	46-PPPPRVP-52		32-PRTSPE-37
	XXX[S/T]PXX		81-KLSSPR-86
	13-PANSPEA-19		103-AQASPP-108
	32-PRTSPEQ-38		143-RNNTPV-148
	81-KLSSPRA-87		
	103-AQASPPP-109		
	143-RNNTPVV-149		

3.2 Expression, trafficking and glycine uptake of *N*-terminus GlyT2 deletion mutants

The sequence analysis and prediction of secondary structure for GlyT2 clearly suggest the presence of a longer *N*-terminal domain for all known vertebrate GlyT2 transporters. Surprisingly, this long domain appears to be absent in invertebrate glycine transporters and its origin and function remain unknown (41). To gain insight into the functional role of the GlyT2 *N*-terminal domain and the possible role of the putative motifs in post-translational modifications such as phosphorylation and ubiquitination, we used the human GlyT2 cDNA as template to generate sequential deletions of this *N*-terminus, which were cloned into pcDNA 3.1 vector containing Flag and His (FH)-epitope tags and resulting in the following constructs: FH-GlyT2 (Full length transporter), partial deletions FH-GlyT2- Δ 43, FH-GlyT2- Δ 109, FH-GlyT2- Δ 157, or complete deletion of the *N*-terminus FH-GlyT2- Δ 201 (Fig. 1B). These short Flag, His-epitopes were placed at the *N*-terminus of each protein to facilitate purification and because they have been shown not to affect the functional properties of other proteins from the *SLC6* transporter family, including DAT and GlyT1

(18,21,42). In addition, we also generated a chimeric construct, FH-1b Δ T2 mutant, in which the GlyT2 *N*-terminus was replaced by the corresponding *N*-terminal tail of human GlyT1b. The wild-type, deletion mutants and chimeric transporter were expressed stably in PAE cells, and the expression and localization analyzed by western blotting and fluorescence microscopy, respectively. For expression, cells from each stable cell line were lysed and transporter purified by His and Flag-affinity chromatography followed by western blotting and detected with Flag antibodies. As shown in the immunoblots of Fig. 1C and D, wild-type and all of the mutants appeared as two immunoreactive bands; a low molecular weight band (~75-45 kDa) corresponding to newly synthesized transporter in the ER, which most likely represent non-glycosylated transporter (*ng*-GlyT2). In addition, it was detected a higher molecular weight band corresponding to the fully glycosylated, mature plasma membrane transporter, that migrated at the predicted size for each polypeptide: ~110 kDa, FH-GlyT2; ~95 kDa, FH-GlyT2- Δ 43; ~80 kDa, FH-GlyT2- Δ 109; ~75 kDa, FH-GlyT2- Δ 157 and ~74 kDa, FH-1b Δ T2 (Fig 1C). Interestingly, deletion of the entire *N*-terminus (FH-GlyT2- Δ 201) resulted in a mature glycoprotein that

migrated as a band with an apparent mass of ~60 kDa, (Fig. 1D). The same results were obtained with an antibody directed against a peptide from the C-terminus of the rat GlyT2

which shows high specificity for the human, rat and mouse transporter (C-GlyT2 antibody, used for figures 2-6).

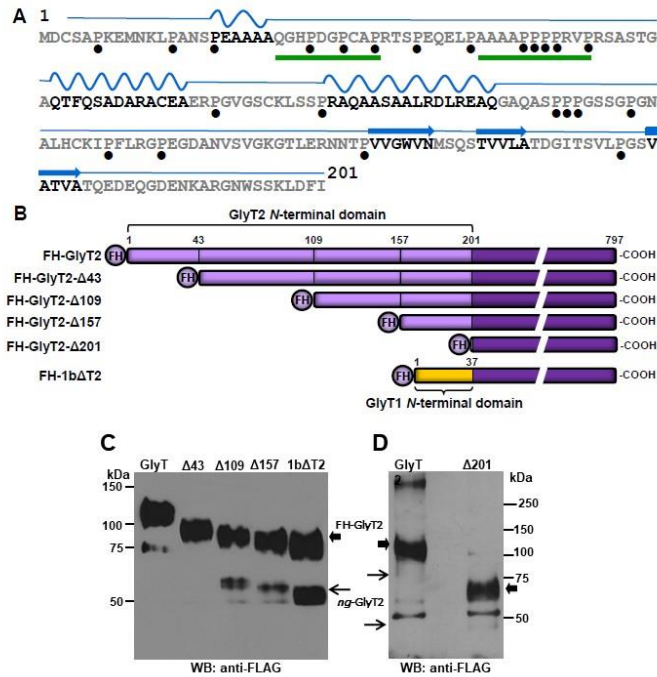


Figure 1. Amino acid sequence of the human GlyT2 N-terminus and GlyT2 expression. (A) The primary amino acid sequence of the GlyT2 N-terminus was subjected to prediction of secondary structure and linear motifs, PSIPRED, PHD, GOR, NPSA and Porter, all available from ExPASy (www.expasy.org). Bold letters indicate regions of α -helix and β -sheet. Straight lines (blue) above the amino acid sequence represent coil regions, curved lines and arrows illustrate α -helices and β -sheets, respectively. The frequency of proline residues, filled black circles; reported phosphosites by 2MS (www.phosphosite.org), red circles; overlapping and non-overlapping non-canonical SH3, WW and proline-directed kinase motifs, green solid bars. (B) Schematic representation of GlyT2 N-terminus deletions tagged with Flag and 10X His (FH) and chimeric protein replacing the GlyT2 N-terminus by the corresponding GlyT1 N-terminus (yellow). (C) PAE cells expressing wild-type FH-GlyT2 or mutant transporters ($\Delta 43$, $\Delta 109$, $\Delta 157$ and chimeric transporters) or (D) mutant FH-GlyT2- $\Delta 201$ were lysed and transporter purified with Ni-NTA agarose and Flag affinity chromatography. Purified proteins were subjected to SDS-PAGE followed by western blotting with Flag antibody. Non-glycosylated transporter, *ng-GlyT2*.

To further investigate the localization of these mutants and the effects of PKC activation on trafficking, wild-type or GlyT2 N-terminus mutants were immunostained with the C-GlyT2 antibody and analyzed by microscopy. The C-GlyT2 has been shown to provide high specificity of detection by both western blot and immunofluorescence

(24,43). As expected, consistent with the results of the western blot that suggested complete maturation of GlyT2 (Fig. 1C), immunostaining of the full length GlyT2 in DMSO-treated cells showed the majority of transporter localized at the plasma membrane (pointed by arrowheads). We also observed some intracellular staining around the

nucleus, representing transporter in the ER in transit to the plasma membrane, corresponding to the non-glycosylated form (Fig. 2A, top panel). The results of immunofluorescence and microscopy showed that mutant transporters with different deletions of the *N*-terminus (Δ 43-201) were localized to the plasma membrane in the vehicle (DMSO)-treated PAE cells, confirming that these represented fully mature, glycosylated transporter (see insets). For simplicity, the mutant FH-GlyT2- Δ 43

was not presented because the phenotype is identical to the wild-type. In some cells, transporter accumulation was detected around the nucleus, likely in the ER, with this pattern of localization being more pronounced in the FH-GlyT2- Δ 157 and FH-GlyT2- Δ 201 deletions. These transporters were localized mostly at the plasma membrane in vehicle treated cells since poor co-localization was observed with the EEA1, which label a specific protein marker of early endosomes (Fig. 2A, inset).

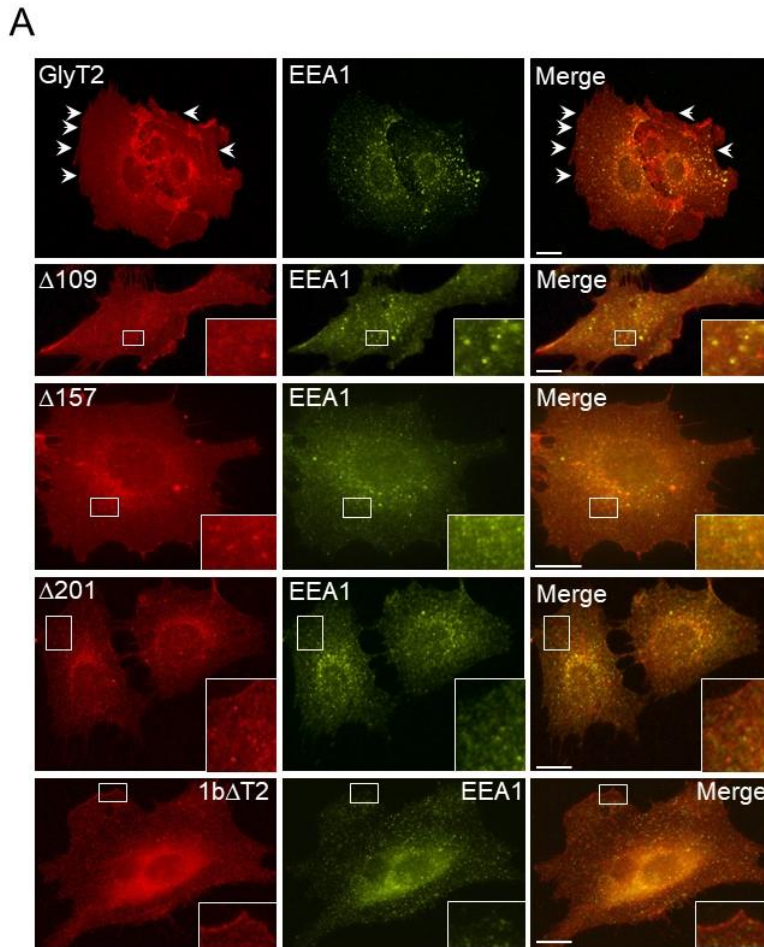


Figure 2. Subcellular localization of GlyT2 transporter and its deletion mutants in PAE cells. PAE cells stably expressing FH-GlyT2, FH-GlyT2 Δ 109, FH-GlyT2 Δ 157, FH-GlyT2 Δ 201 or FH-1b Δ GlyT2 were incubated with 0.01% DMSO (A) or 1 μ M PMA (B) for 30 min at 37 °C, fixed with 4% paraformaldehyde, and stained with C-GlyT2 (antibodies against the C-terminus) and EEA1 antibodies followed by incubation with Cy3 (red) and Alexa-488 (green) conjugated secondary antibodies, respectively. Nuclei were labeled with DAPI (blue). *Scale bar: 10 μ m.*

We, and others, have previously reported that all GlyT1 isoforms and GlyT2 undergo endocytosis after PKC activation by PMA (12,18,20). To investigate a possible role of the *N*-terminus in the PKC-dependent GlyT2 endocytosis, we incubated cells expressing the full length GlyT2 or its deletion mutants with phorbol ester (PMA) for 30 min and analyzed endocytosis of GlyT2 by co-localization with the EEA1 marker. As illustrated in Fig. 2B, PKC activation by PMA triggered trafficking of the full length GlyT2 from the plasma membrane, where it appeared barely visible, into early endosomes as shown by co-localization of a large population of endosomes with EEA1. Similarly, the indicated GlyT2 deletion mutants and 1bΔT2 chimera were all internalized into EEA1 positive endosomes after PKC activation (Fig. 2B, insets). These results together suggest that the deletion of GlyT2 *N*-terminal residues 1-201 do not affect anterograde or retrograde trafficking, or the PKC response. Trafficking to the plasma membrane is a critical step for GlyT2 function given that glycine uptake is dependent on the sodium gradient generated by the plasma membrane Na⁺/K⁺-ATPase. To determine the effects of the *N*-terminal deletions on the kinetic parameters *K_m* and *V_{max}* and their response to PKC activation, we measured glycine transport for the wild-type and GlyT2

deletion mutants. As shown in Table 3, when cells expressing the wild-type or mutants were incubated with vehicle DMSO, all of them were able to bind and translocate glycine with *V_{max}* constants ranging from 4.4-8.9 nmol/min/mg. These values demonstrate that the deletion mutants reach the plasma membrane and that removal of the *N*-terminus does not significantly impact the activity. Moreover, incubation of cells expressing the wild-type GlyT2 with 1 μM PMA for 30 min led to a consistent ~40-50% reduction in *V_{max}* compared to DMSO-treated cells. A similar reduction in *V_{max}* was observed for the deletion mutants of Δ43 and Δ109 amino acids followed by deletions Δ157 and Δ201 (~60-65 % reduction). The largest change was observed for the chimeric protein FH-1bΔT2, where a consistent ~70-80% decreased *V_{max}* value was obtained. Not surprising, the *K_m* values measured for the wild-type and mutants did not vary significantly under DMSO and PMA conditions, demonstrating that the decreased in *V_{max}* was likely due to endocytosis (Table 3). These data together suggest that the first 201 amino acids of the GlyT2 *N*-terminal tail are not critical for substrate recognition and translocation; however, PMA-treatment for deletions of 157-201 led to significant reductions in *V_{max}* values, pointing to the *N*-terminus as a domain important for retrograde trafficking.

Table 3: Kinetic properties of the wild typehGly12 and N-terminal deletions

Transporter	<i>V_{max}</i>		<i>K_m</i>	
	(nmol/min/mg)		μM	
	DMSO	PMA	DMSO	PMA
FH-GlyT2	7.5±1.2	4.3±1.4	106±14	113±19
Δ43	8.9±1.2	4.8±1.2	121±17	92±22
Δ109	6.1±0.5	4.5±0.9	113±23	134±22
Δ157	5.1±0.4	2.1±0.2	225±17	196±25
Δ201	4.4±0.5	1.6±0.4	249±19	264±18
1b ΔT2	5.9±1.1	1.4±0.2	152±22	135±25

Table 3: PAE cells stably expressing the human GlyT2 or mutants were incubated with DMSO or 1 μM PMA for 30 min followed by glycine uptake. The assay was performed as described in “experimental procedures”. Kinetic parameters were calculated using the *Michaelis-Menten* equation and sigma plot 11. Values represent the mean of at least 3 determinations \pm SE.

3.3 Phosphorylation and ubiquitination of GlyT2

The GlyT2 N-terminus contains several consensus sequences for recognition and modification by different protein kinases, including proline-directed kinases such as MAPK and phosphatases like PP1 (Fig. 1A, Table 2). However, to date there is no published evidence to demonstrate that GlyT2 is a phosphoprotein. In addition, several lysine residues are spread throughout this domain, pointing to this tail as a potential target for other post-translational modifications. To examine whether GlyT2 was phosphorylated in a PKC-dependent manner, we incubated cells with vehicle DMSO or with 1 μM PMA and performed metabolic labeling experiments. As shown by

incorporation of [³²P]-orthophosphate in Fig. 3A, GlyT2-expressing cells incubated with vehicle showed basal levels of phosphorylation which dramatically increase about 5-fold in the first 15 min of PMA incubation and were maintained at the higher levels even after 2 h incubation. The PKC-dependency of GlyT2 phosphorylation was demonstrated by a 30 min pre-incubation of the cells with the PKC inhibitor BIM followed by 2 h PMA treatment, this resulted in abolishment of the PKC-dependent GlyT2 phosphorylation (Fig 3A-B). To our knowledge, this is the first direct experimental evidence to demonstrate that GlyT2 is a phosphoprotein and that phosphorylation can be regulated by PKC activation.

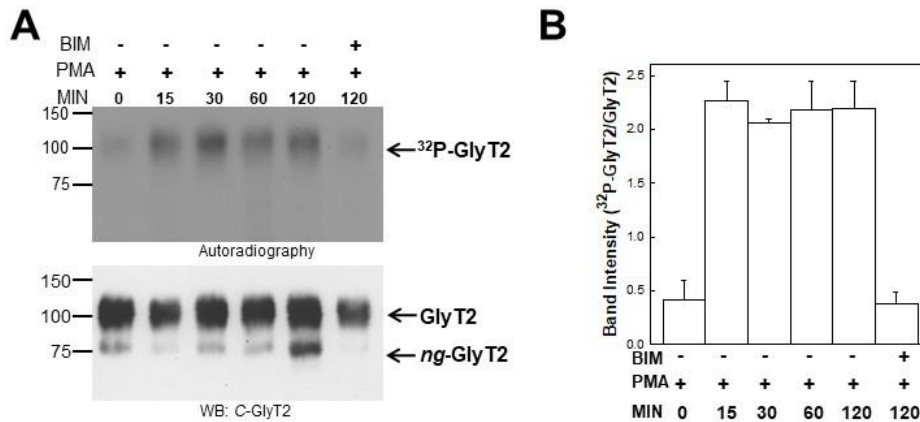


Figure 3. Enhanced GlyT2-phosphorylation in response to PKC activation. (A) PAE cells expressing wild-type GlyT2 were labeled with 0.125 mCi [³²P]-orthophosphate/well as described in “Experimental Procedures” followed by incubation with 1 μM PMA for 0-120 min, or 1 μM BIM followed by the addition of 1 μM PMA. Labeled GlyT2 was purified by tandem affinity chromatography and analyzed by autoradiography and western blotting with GlyT2 antibodies against the *N*-terminus. (B) The bar graph shows a quantitative plot of phosphorylated GlyT2 normalized by the total GlyT2 (mean±SE, n=3).

Given that the wild-type GlyT2 phosphorylation state is maintained from 15-120 min after PKC activation, we analyzed the levels of phosphorylation of the deletion mutants after 30 min incubation with PMA. As depicted in Fig 4A, the Δ43 and Δ109 deletion mutants showed similar phosphorylation levels, under unstimulated conditions, to those observed for the wild-type. However upon PKC-stimulation, the Δ43 and Δ109 mutants exhibited an increment in phosphorylation signal that total 60-70% of the levels observed for the wild-type GlyT2 protein (Fig. 4A). Different behavior was observed for the mutants FH-GlyT2-Δ157 and FH-GlyT2-Δ201, where in non-stimulated cells, the mutant proteins showed steady-state phosphorylation levels lower than those obtained for the wild-type GlyT2. A more dramatic change was

observed for these mutants after PMA stimulation, where PKC-dependent phosphorylation was greatly diminished or completely abolished, suggesting that several phosphorylation sites, if not all of them, are located within the first 157 amino acids of the *N*-terminus (Fig. 4A, B). The sequence analysis for the GlyT2 *N*-terminus shown in Figure 1A confirms the presence of 21 serine and 10 threonine residues, many of which are predicted potential phosphorylation sites by different kinases, including PKC (Fig. 1A). Of these, 16 serine and 5 threonine residues were eliminated in the FH-GlyT2-Δ157 mutant or removal of all of them for the mutant FH-GlyT2-Δ201 (Fig. 4C). Interestingly, the *C*-terminus contains only 3 serine and 2 threonine residues (data not shown) that do not appear to contribute to the overall PKC-dependent GlyT2 phosphory-

lation. To provide solid support of our results, we looked for phosphorylation sites identified by high-throughput tandem MS experiments, published in the PhosphoSite Plus, a knowledge database reporting one-third of a million non-redundant modification sites on proteins from mouse, rat and human (www.phosphosite.org, (44)). Strikingly, several phosphorylation sites have been identified at the *N*-terminus of the human GlyT2, corresponding to Ser56, Thr57 and Ser84, recorded multiple times with 2, 4 and 5 hits respectively. In addition, Thr61, Ser83 and Ser91 have been reported as one-hitters

but a $p < 0.05$, suggesting that these phosphosites may be potentially real. Not surprising, the corresponding sites in the rat and mouse GlyT2 have been also identified as phosphorylation sites. Consistent with our hypothesis that the *C*-terminus does not contribute to GlyT2 phosphorylation, no phosphorylation sites have been identified or reported in the PhosphoSitePlus database for the *C*-terminus. These PhosphoSitePlus MS2 data provide evidence that multiple phosphorylation sites lie within the *N*-terminus.

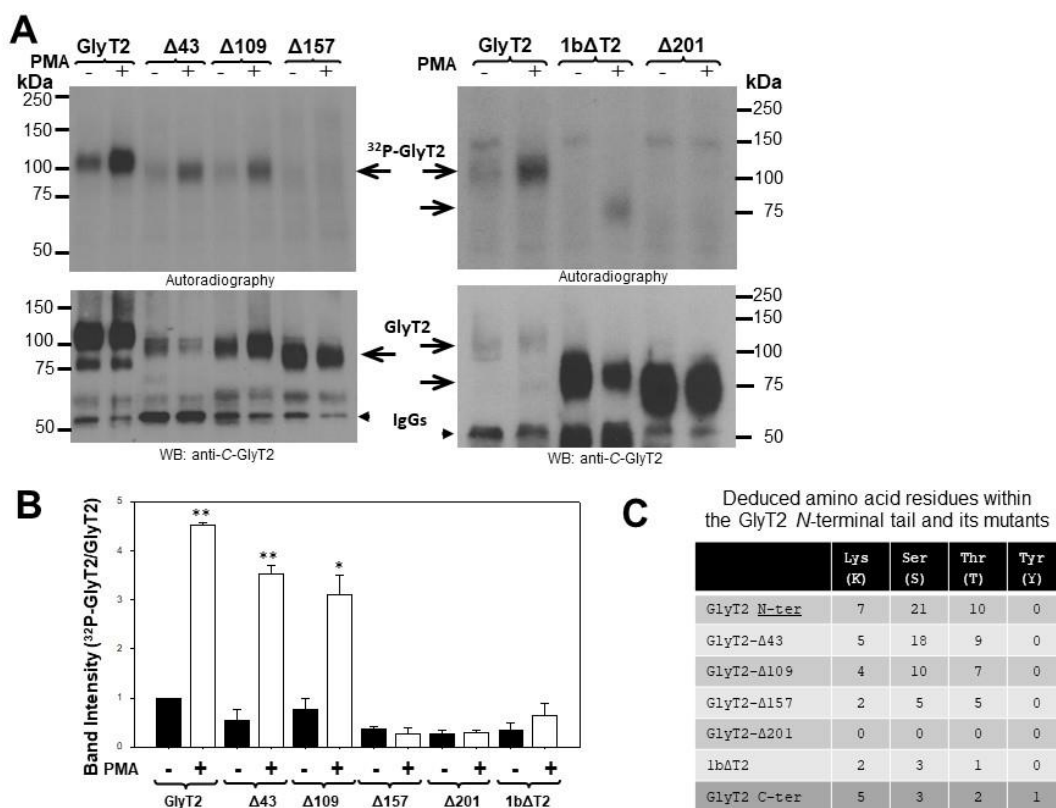


Figure 4. PKC-dependent phosphorylation of *N*-terminus deletions. (A) PAE cells stably transfected with either pcDNA3.1, FH-GlyT2, FH-GlyT2Δ43, FH-GlyT2Δ109, FH-GlyT2Δ157 or FH-1bΔGlyT2 and FH-GlyT2Δ201 were incubated with 125 μCi [³²P]-orthophosphate/ml for 2 h, followed by incubation with DMSO or 1 μM PMA for 30 min. Labeled GlyT2 was purified by tandem affinity chromatography and analyzed by autoradiography and western blotting (WB) with guinea pig c-GlyT2 antibodies. Phosphorylated GlyT2, ³²P-GlyT2; Immunoglobulin, IgG. (B) Quantification of phosphorylated GlyT2 normalized by total GlyT2 using ImageJ software (mean SE, n=3). Statistical analysis was performed using one-way ANOVA: * $p < 0.05$ and ** $p < 0.01$. (C) Quantity of lysine, serine, threonine and tyrosine residues along the *N*- and *C*-terminus of the human GlyT2 transporter and deletion mutants.

Interestingly, a modest increase in PKC-dependent phosphorylation levels was observed for the chimeric transporter FH-1b Δ T2 (Fig 4A-B). The human GlyT1 *N*-terminus contains three serines and one threonine residues, indicating that any of these residues represent potential phosphorylation sites and may account for this increased level of PKC-dependent phosphorylation. In agreement with the results for the chimeric transporter, NetPhos 2 server analysis of phosphorylation sites for the human GlyT1b *N*-terminus suggest the presence of two potential phosphorylation sites, depicting a score close to 1.0 (www.cbs.dtu.dk/service/NetPhos). These sites correspond to the amino acids 7-PVAPSSPEQN-16 and 20-PSEATKRDQ-28, pointing to Ser-12 and Thr-24 residues as the potential phospho-sites in the chimeric transporter. Not surprising, Ser-21 and Thr-24 has been reported to be phosphorylated by High-Throughput tandem mass spectrometry in human, rat and mouse GlyT1 isoforms (www.phosphosite.org, (44)), in agreement with Netphos prediction.

PKC activation has also been shown to induce ubiquitination of GlyT2 (45). It was reported that Lys-791 located at the *C*-terminus of the rat GlyT2 serves as the main ubiquitin conjugation site in response to PKC activation, whereas the four *C*-terminal

lysine residues were reported to be responsible for constitutive endocytosis (45,46). To investigate whether the *N*-terminal deletion mutants affected the overall transporter ubiquitination, we incubated cells expressing wild-type GlyT2 or the deletion mutants with DMSO or 1 μ M PMA for 30 min followed by transporter purification, SDS-PAGE and western blotting with ubiquitin and *C*-GlyT2 antibodies. As shown in Fig. 5A, protein purification from control PAE cells transfected with pCDNA did not show any immunoreactive band. In the other hand, when cells expressing transporters were stimulated with PMA and purified transporter subjected to western blotting, it resulted in a dramatic 5-7 fold increase in ubiquitination over that observed for DMSO-treated cells. This pattern was observed for wild-type GlyT2 as well as the Δ 43, Δ 109 and Δ 157 mutants. Although all of the mutants resulted in similar levels of enhanced ubiquitination in response to PKC activation, we observed that gradual deletion of the *N*-terminus led to an increase in the levels of constitutive and PKC-dependent ubiquitination, more markedly detected for the deletion FH-GlyT2- Δ 157 and the chimeric transporter (Fig. 5A and B). Similar behavior to FH-GlyT2- Δ 157 was observed for the mutant FH-GlyT2- Δ 201 (Not shown).

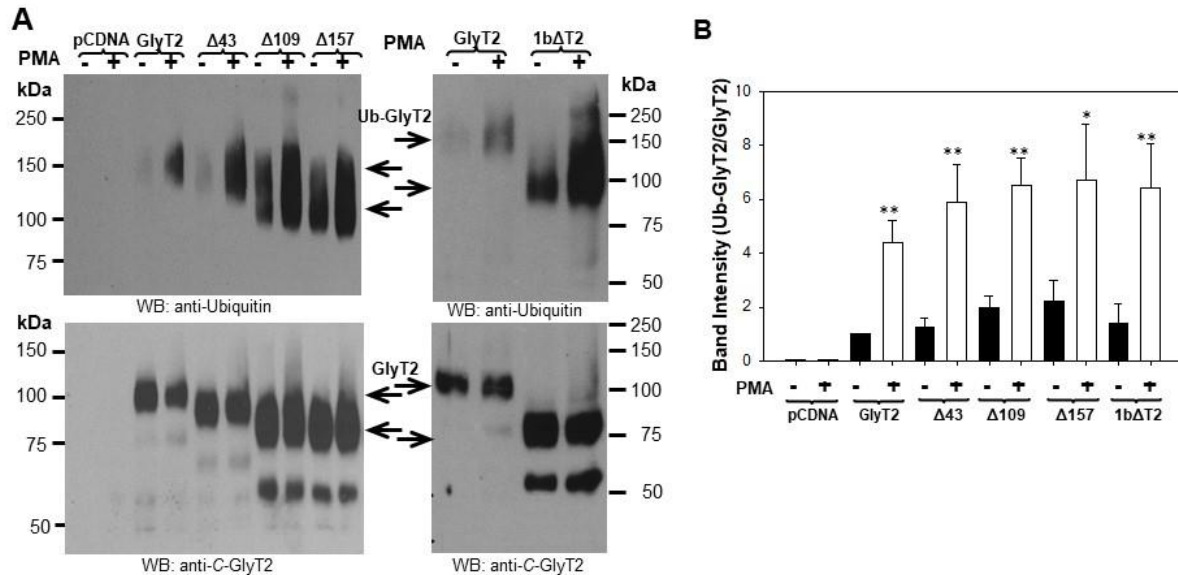


Figure 5. PKC-dependent ubiquitination of N-terminus deletions. (A) PAE cells stably expressing FH-GlyT2, FH-GlyT2 Δ 43, FH-GlyT2 Δ 109, FH-GlyT2 Δ 157 or FH-1b Δ GlyT2 were treated with DMSO or 1 μ M PMA for 30 min at 37 °C. Following PMA incubation, GlyT2 was purified by tandem affinity chromatography and analyzed by western blotting with ubiquitin and GlyT2 antibodies against the C-terminus (c-GlyT2). Ubiquitinated GlyT2, *Ub-GlyT2*. (B) Quantification of ubiquitinated GlyT2 normalized by total GlyT2 using ImageJ software (mean SE, n=3-4). Statistical analysis was performed using one-way ANOVA: * p <0.05 and ** p <0.01.

3.4 Enhanced GlyT2 degradation by deletion of the N-terminus

We have previously provided solid evidence for GlyT1 and DAT demonstrating that transporter ubiquitination serves as a signal for endocytosis and sorting into lysosomes (21,42,47). To examine the rate of degradation triggered by PKC activation, cells expressing wild-type GlyT2 and its deletion mutants were treated with cycloheximide (CHX) for 2 h to inhibit protein synthesis, eliminating the presence of newly synthesized GlyT2 protein in the cell. The 2 h CHX treatment allows transporter in the ER to mature and traffic to the plasma membrane. Following CHX treatment, the cells were incubated with DMSO for 6 h or 1 μ M PMA for 0-6 h, lysed and the total lysates subjected to separation via SDS-PAGE and western blotting with C-GlyT2 and actin

antibodies. As shown in Figure 6A, PMA treatment of the wild-type GlyT2 expressing cells resulted in down-regulation of the transporter with a half-life time of 6 h, after normalization with β -actin, which was used as loading control. Treatment of the cells with vehicle DMSO for 6 h did not show any statistically significant change in the total transporter levels, as compared to untreated cells which were exposed only for 2 h to CHX (Fig 6A, first, second and last lane). Similar behavior to the wild-type was observed for the deletion mutant of the first 43 amino acids (GlyT2- Δ 43; data not shown). By contrast, for the mutant FH-GlyT2- Δ 109 (similarly for FH-GlyT2- Δ 157 and FH-GlyT2- Δ 201, data not shown), PMA exposure led to a reduction in the half-life of the transporter to \sim 3 hours, representing faster turnover compared to the wild-type

protein, probably by exposing potential ubiquitination sites. Consistent with a faster turnover for these transporters, increased degradation was also observed after 6 h of vehicle DMSO treatment compared to a 0 h time-point, a change not observed for the wild-type (Fig. 6B, compare first and last lanes). The most dramatic change was observed for the chimera FH-GlyT2-1bΔT2, where PMA treatment induced a faster degradation, exhibiting a half-life of only 0.5-1 h (Fig. 6C). Strikingly, the turn over for this chimera was accelerated even in the

absence of PMA, displaying a half-life of 1-2 h in DMSO-treated cells. These findings suggest that a gradual deletion of the GlyT2 *N*-terminal cytoplasmic domain results in enhanced ubiquitination, increased instability of GlyT2 at the plasma membrane and faster turnover. Moreover, we can speculate that a potential interaction of the *N*-terminus with the *C*-terminus domain takes place and that deletion of the *N*-terminus increases exposure of ubiquitination sites at the *C*-terminus, resulting in a gradual increased transporter ubiquitination and degradation.

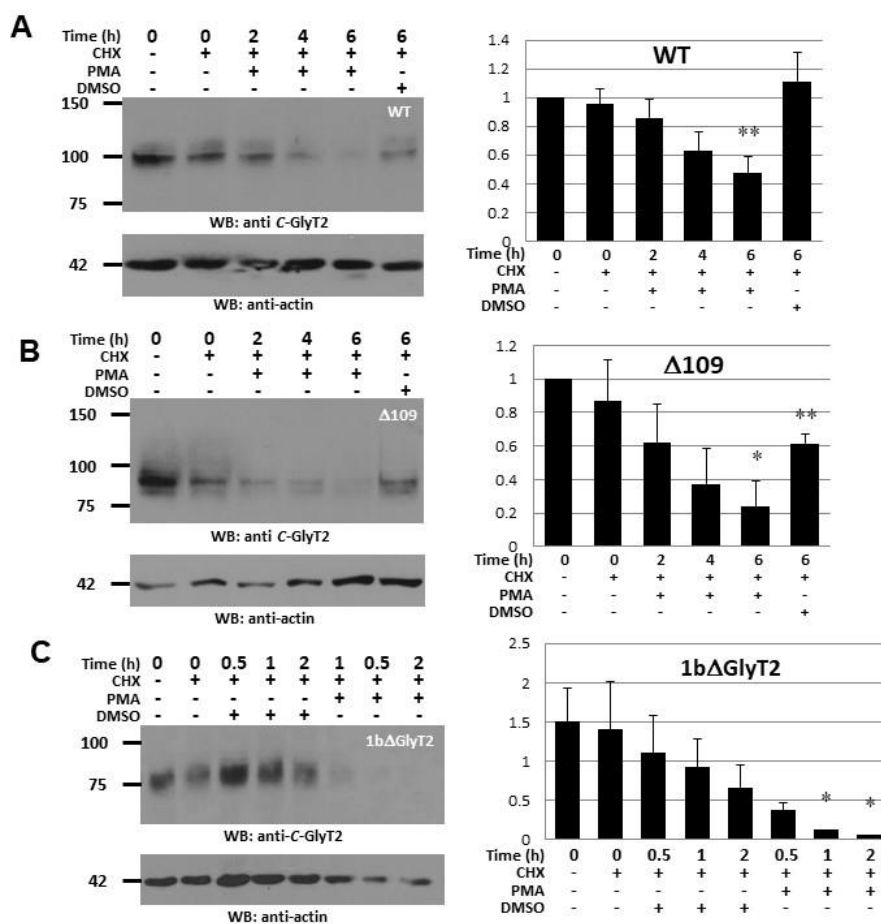


Figure 6. PKC-dependent GlyT2 degradation. PAE cells expressing (A) wild type FH-GlyT2, (B) mutant FH-GlyT2Δ109 or (C) FH-1bΔGlyT2 were incubated with 50 μg/ml of cycloheximide (CHX) for 2 h followed by treatment with DMSO or 1 μM PMA for 6 h, 4 h, or 2 h, respectively. Additional 1 h and 30 min time-points were assayed for FH-1bΔGlyT2. After incubation, the lysates were subjected to SDS-PAGE and western blot with *C*-GlyT2 and anti-actin antibodies. The results are from three independent experiments, and statistical analysis was performed using one-way ANOVA: * $p < 0.025$; ** $p = 0.005$

4. Discussion

The vertebrate nervous system utilizes glycine transporters GlyT1 and GlyT2 to clear the neurotransmitter glycine from the synaptic cleft to terminate neurotransmission. In spite of the high homology among GlyT sequences, the mammalian GlyT2 transporter is characterized by a unique long *N*-terminal domain of unknown function. Homology searches using different algorithms suggest that the *N*-terminus of GlyT2 is unique, given that no homology has been found for any gene product in the protein data bank. We therefore believe that this *N*-terminus appeared during the transition of invertebrates deuterostomes to vertebrates due to functional specialization, pointing to this domain as a good candidate to study (48). Based on the sequence analysis presented in Figure 1, we propose that this domain contains modules that mediate interaction with other proteins to regulate post-translational modifications and thereby regulating several aspects of transport and protein trafficking. It is of interest that the bioinformatics analysis of the *N*-terminal amino acid sequence shown in Figure 1 uncovered interesting features that may provide insights into the potential functions of this domain. First, the presence of several proline residues spread throughout the *N*-terminus indicated a poorly structured domain, most likely a coil region, which is consistent with predictions by several secondary structure algorithms. These algorithms predicted a region of mostly coiled stretches and three short (5-7 residues) α -helices. Secondly, several of these prolines appear clustered in proline-rich motifs (PRM), creating five consensus sites for proline-directed kinases (XXX[s/t]PXX) that may play a role in GlyT2 stability and trafficking. In line with a potential role of these proline-directed kinases on GlyT2 phosphorylation, our results demonstrate the

presence of serine/threonine phosphorylation sites within the first 157 amino acids at the *N*-terminus, given that removal of this stretch of residues greatly diminished the PKC-dependent phosphorylation. It is worth mentioning that this stretch is devoid of tyrosines but contain 21 serine and 10 threonine residues, indicating that PKC-dependent GlyT2 phosphorylation must be at these amino acids. Consistent with this notion, Ser-83 and 84 within the PRM 81-KLSSPRA-87 has been shown to be phosphorylated by tandem MS, in addition to other Ser, Thr residues within the first 100 amino acids of the *N*-terminus. Moreover, our previous studies on GlyT1 and others on the dopamine transporter demonstrate that PKC-dependent phosphorylation takes place at serine/threonine residues, supporting the possible role of proline-directed kinases for Ser/Thr GlyT2 phosphorylation (18,40,49). Interestingly, the deletion of the first 109 amino acids eliminates four of these motifs and the levels of PKC-dependent GlyT2 phosphorylation was diminished by 50% (Fig. 5). Further removal of an additional forty eight amino acids (GlyT2- Δ 157), encompassing the fifth motif, resulted in a dramatic reduction of the PKC-dependent phosphorylation, compared to the levels observed for the GlyT2 wild type protein, supporting the role of these motifs in GlyT2 phosphorylation. A remarkable similar mechanism has been well documented for the Glycine receptor GlyR-gephyrin protein complex. The microtubule binding protein gephyrin contains a PRM (LP(S)PPPP) that undergoes proline-directed phosphorylation at the serine residue within the motif followed by binding of the prolyl *cis/trans* isomerase Pin1, which induces a conformational change on phospho Ser-Pro motif of gephyrin to increase its affinity for the beta subunit of GlyR (50). It is therefore postulated that this interaction increases the stability and localization of GlyRs to synaptic

sites. By contrast, phosphorylation of Ser403 located within the cytoplasmic domain of the GlyR beta subunit reduced the binding affinity between the complex, leading to diffusion of GlyRs to extrasynaptic sites [(51), reviewed in (52)]. It is possible that this postsynaptic mechanism could take place for presynaptic proteins.

Based on the presence of several Ser-Pro motifs encompassing the GlyT2 *N*-terminus and our observation that PKC-dependent phosphorylation takes place in this domain, we postulate that any of these Proline-directed kinase motifs may direct Ser/Thr phosphorylation and serve to recruit relevant protein-protein interactions that modulate GlyT2 localization and intracellular trafficking. For example, the *N*-terminus may serve to connect GlyT2 to the cytoskeleton and regulate localization to synaptic sites. Similar proline-rich regions are found in the WH2 domain of the WASP and N-WASP proteins, which confers binding to actin (53,54). In addition, the linear motif prediction algorithm also identified six WW motifs and four non-canonical SH3 motifs within the human GlyT2. Interestingly, five of the predicted WW motifs (class IV) converge with the proline-directed kinase motifs, consistent with the fact that group IV WW domains recognize phospho-ser or phospho-thr followed by a proline residue, in a phosphorylation dependent manner (34,55). Not surprising, the prolyl isomerase Pin1 contains a WW domain that binds the pSer-Pro motif of gephyrin, to catalyze the isomerization of the proline and trigger conformational changes (50). In line with our hypothesis that proline-directed kinase and WW domains may play a role in GlyT2 trafficking, our results demonstrate for the first time that PKC activation triggers GlyT2 phosphorylation and these phosphorylation sites lie within the first 157 residues of the *N*-

terminus, a region shown to contain all of these motifs.

Another aspect of our current study is to highlight that multiple residues within the *N*-terminus are likely to be phosphosites, given that the deletion of the first 43 amino acids led to a partial reduction in the phosphorylation levels and these were only abolished after deletion of the first 157 amino acids. Not surprising, multiple serine and threonine residues within the *N*-terminus have been identified as phosphosites by HTP mass spectrometry (www.phosphosite.com). The presence of several phosphorylation sites and motifs along GlyT2 *N*-terminus could serve as recognition sites within the context of multiple molecular scenarios. We can speculate that GlyT2 localization and stability are likely regulated by numerous factors, including the interaction of a kinase to phosphorylate ser/thr residues and recruitment of actin binding proteins carrying WW domains. These motifs may also serve to bring E3 ligases in close proximity to its target residues, thereby ultimately resulting in phosphorylation and ubiquitination of GlyT2. It was previously shown that rat GlyT2 is ubiquitinated in response to PKC activation at a single lysine residue Lys-791 located at the *C*-terminal tail followed by endocytosis (45). In addition, the same group reported that constitutive endocytosis is dependent on ubiquitination of a cluster of lysines at the same location (46).

We showed that deletion of 157 or 201 *N*-terminal residues abolished phosphorylation but did not affect ubiquitination. Not surprising, ubiquitination has been detected by MS at the four lysine residues within the *C*-terminus of the human GlyT2. It is possible that other motifs located within the *C*-terminus may serve as binding sites for interacting proteins. For example, the last three residues of the *C*-terminus form

a type III PDZ site shown to bind the PDZ domain of Syntenin-1, an interaction that results in trafficking and stabilization of GlyT2 at synaptic sites (23,24). Interestingly, several plasma membrane transporters including the cationic amino acid (CAT-1), the dopamine (DAT) and glutamate (GLT-1) transporters are Lys63-linked poly-ubiquitinated by the HECT-containing domain E3 ligase NEDD4-2, in response to PKC activation (39,56,57). The Nedd4 family members are characterized by the presence of a calcium/lipid binding C2 domain, the HECT ligase domain and between 2-4 WW domains that play a major role in substrate binding (58). The GlyT2 C-terminal domain carries the sequence CSPQP that represent a type IV WW motif. Worth mentioning is that these Nedd4 WW domains have been shown to bind peptides containing the pS/T(P), (L/P)PXY motifs, suggesting that GlyT2 WW motif may be potential binding sites for Nedd4 family members (59). Moreover, Nedd4-2 carrying mutations of WW3 and WW4 domains impaired the PKC-dependent DAT ubiquitination, suggesting an unconventional binding of Nedd4-2 to DAT, independent of PPXY. Similar unconventional E3 ligase binding may also occur for GlyT2. Although future mutagenesis and protein-protein interaction studies are needed to elucidate the precise role of the motifs located in the GlyT2 N-terminus domain, the data presented in this study supports the merging concept that GlyT2 N-terminus functions as a scaffold that contributes to multiple dynamic processes such as GlyT2 subcellular localization and stabilization. Future studies in an endogenous system will likely integrate this novel concept to the mechanism of presynaptic

scaffold and regulation of glycinergic neurotransmission. Moreover, understanding molecular details of GlyT2 trafficking, subcellular localization and anatomy of GlyT2-containing neuronal circuits, could contribute towards potential drug discovery to improve the neurological disorders in hyperekplexia-afflicted patients.

5. Conclusions

In summary, we demonstrated that sequential deletions at the N-terminus of the GlyT2 did not affect PKC-dependent ubiquitination; however, deletion of 157 or 201 N-terminal residues abolished phosphorylation. In addition, glycine uptake was not abolished by the N-terminal deletions but affected the stability of transporter at the plasma membrane. These observations together point to the N-terminus as an intracellular domain critical for transporter localization at the plasma membrane, possibly as part of an intracellular scaffold complex.

Acknowledgements

We thank the staff of the Imaging and the Genomic Analysis Core Facilities for services and facilities provided. This study was supported by grant NIMH 5SC1MH 086070-04 to MM and also in part by the grants DA029989 to Dr. Edward Castaneda. MP was supported by a fellowship from the MARC-U-STAR Undergraduate Biomedical Research Training 2T34GM008048. We also thank Drs. Giulio Francia and Das Siddhartha for critical reading of the manuscript and helpful suggestions and Ms. Ana Betancourt for DNA sequencing.

References

1. Coleman, W. L., Fischl, M. J., Weimann, S. R., and Burger, R. M. (2011) GABAergic and glycinergic inhibition modulate monaural auditory response properties in the avian superior olivary nucleus. *J Neurophysiol* **105**, 2405-2420
2. Liu, Q. R., Lopez-Corcuera, B., Mandiyan, S., Nelson, H., and Nelson, N. (1993) Cloning and expression of a spinal cord- and brain-specific glycine transporter with novel structural features. *J Biol Chem* **268**, 22802-22808
3. Morrow, J. A., Collie, I. T., Dunbar, D. R., Walker, G. B., Shahid, M., and Hill, D. R. (1998) Molecular cloning and functional expression of the human glycine transporter GlyT2 and chromosomal localisation of the gene in the human genome. *FEBS Lett* **439**, 334-340
4. Gether, U., Andersen, P. H., Larsson, O. M., and Schousboe, A. (2006) Neurotransmitter transporters: molecular function of important drug targets. *Trends in Pharmacological Sciences* **27**, 375-383
5. Aragon, C., and Lopez-Corcuera, B. (2003) Structure, function and regulation of glycine neurotransmitters. *Eur J Pharmacol* **479**, 249-262
6. Eulenburg, V., Armsen, W., Betz, H., and Gomeza, J. (2005) Glycine transporters: essential regulators of neurotransmission. *Trends Biochem Sci* **30**, 325-333
7. Gomeza, J., Ohno, K., Hulsmann, S., Armsen, W., Eulenburg, V., Richter, D. W., Laube, B., and Betz, H. (2003) Deletion of the mouse glycine transporter 2 results in a hyperekplexia phenotype and postnatal lethality. *Neuron* **40**, 797-806
8. Szoke, K., Hartel, K., Grass, D., Hirrlinger, P. G., Hirrlinger, J., and Hulsmann, S. (2006) Glycine transporter 1 expression in the ventral respiratory group is restricted to protoplasmic astrocytes. *Brain Res* **1119**, 182-189
9. Zafra, F., Aragon, C., Olivares, L., Danbolt, N. C., Gimenez, C., and Storm-Mathisen, J. (1995) Glycine transporters are differentially expressed among CNS cells. *J Neurosci* **15**, 3952-3969
10. Lee, E. J., Mann, L. B., Rickman, D. W., Lim, E. J., Chun, M. H., and Grzywacz, N. M. (2006) AII amacrine cells in the distal inner nuclear layer of the mouse retina. *J Comp Neurol* **494**, 651-662
11. Mohler, H., Boison, D., Singer, P., Feldon, J., Pauly-Evers, M., and Yee, B. K. (2011) Glycine transporter 1 as a potential therapeutic target for schizophrenia-related symptoms: evidence from genetically modified mouse models and pharmacological inhibition. *Biochem Pharmacol* **81**, 1065-1077
12. Nunez, E., Perez-Siles, G., Rodenstein, L., Alonso-Torres, P., Zafra, F., Jimenez, E., Aragon, C., and Lopez-Corcuera, B. (2009) Subcellular localization of the neuronal glycine transporter GLYT2 in brainstem. *Traffic* **10**, 829-843
13. Rees, M. I., Harvey, K., Pearce, B. R., Chung, S. K., Duguid, I. C., Thomas, P., Beatty, S., Graham, G. E., Armstrong, L., Shiang, R., Abbott, K. J., Zuberi, S. M., Stephenson, J. B., Owen, M. J., Tijssen, M. A., van den Maagdenberg, A. M., Smart, T. G., Supplisson, S., and Harvey, R. J. (2006) Mutations in the gene

- encoding GlyT2 (SLC6A5) define a presynaptic component of human startle disease. *Nat Genet* **38**, 801-806
14. Eulenburg, V., Becker, K., Gomeza, J., Schmitt, B., Becker, C. M., and Betz, H. (2006) Mutations within the human GLYT2 (SLC6A5) gene associated with hyperekplexia. *Biochem Biophys Res Commun* **348**, 400-405
 15. Harvey, R. J., Topf, M., Harvey, K., and Rees, M. I. (2008) The genetics of hyperekplexia: more than startle! *Trends Genet* **24**, 439-447
 16. Miranda, M., Dionne, K. R., Sorkina, T., and Sorkin, A. (2007) Three Ubiquitin Conjugation Sites in the Amino Terminus of the Dopamine Transporter Mediate Protein Kinase C-dependent Endocytosis of the Transporter. *Mol. Biol. Cell* **18**, 313-323
 17. Dipace, C., Sung, U., Binda, F., Blakely, R. D., and Galli, A. (2007) Amphetamine induces a calcium/calmodulin-dependent protein kinase II-dependent reduction in norepinephrine transporter surface expression linked to changes in syntaxin 1A/transporter complexes. *Mol Pharmacol* **71**, 230-239
 18. Vargas-Medrano, J., Castrejon-Tellez, V., Plenge, F., Ramirez, I., and Miranda, M. (2011) PKCbeta-dependent phosphorylation of the glycine transporter 1. *Neurochem Int* **59**, 1123-1132
 19. Fernandez-Sanchez, E., Martinez-Villarreal, J., Gimenez, C., and Zafra, F. (2009) Constitutive and regulated endocytosis of the glycine transporter GLYT1b is controlled by ubiquitination. *J Biol Chem* **284**, 19482-19492
 20. Fornes, A., Nunez, E., Alonso-Torres, P., Aragon, C., and Lopez-Corcuera, B. (2008) Trafficking properties and activity regulation of the neuronal glycine transporter GLYT2 by protein kinase C. *Biochem J* **412**, 495-506
 21. Barrera, S. P., Castrejon-Tellez, V., Trinidad, M., Robles-Escajeda, E., Vargas-Medrano, J., Varela-Ramirez, A., and Miranda, M. (2015) PKC-Dependent GlyT1 Ubiquitination Occurs Independent of Phosphorylation: Inspecificity in Lysine Selection for Ubiquitination. *PLoS One* **10**, e0138897
 22. Fornes, A., Nunez, E., Aragon, C., and Lopez-Corcuera, B. (2004) The second intracellular loop of the glycine transporter 2 contains crucial residues for glycine transport and phorbol ester-induced regulation. *J Biol Chem* **279**, 22934-22943
 23. Ohno, K., Koroll, M., El Far, O., Scholze, P., Gomeza, J., and Betz, H. (2004) The neuronal glycine transporter 2 interacts with the PDZ domain protein syntenin-1. *Mol Cell Neurosci* **26**, 518-529
 24. Armsen, W., Himmel, B., Betz, H., and Eulenburg, V. (2007) The C-terminal PDZ-ligand motif of the neuronal glycine transporter GlyT2 is required for efficient synaptic localization. *Mol Cell Neurosci* **36**, 369-380
 25. Geerlings, A., Lopez-Corcuera, B., and Aragon, C. (2000) Characterization of the interactions between the glycine transporters GLYT1 and GLYT2 and the SNARE protein syntaxin 1A. *FEBS Lett* **470**, 51-54
 26. Geerlings, A., Nunez, E., Lopez-Corcuera, B., and Aragon, C. (2001) Calcium- and Syntaxin 1-mediated Trafficking of the Neuronal Glycine

- Transporter GLYT2. *J. Biol. Chem.* **276**, 17584-17590
27. Quick, M. W. (2003) Regulating the conducting states of a mammalian serotonin transporter. *Neuron* **40**, 537-549
 28. Binda, F., Dipace, C., Bowton, E., Robertson, S. D., Lute, B. J., Fog, J. U., Zhang, M., Sen, N., Colbran, R. J., Gnegy, M. E., Gether, U., Javitch, J. A., Erreger, K., and Galli, A. (2008) Syntaxin 1A interaction with the dopamine transporter promotes amphetamine-induced dopamine efflux. *Mol Pharmacol* **74**, 1101-1108
 29. Horiuchi, M., Loebrich, S., Brandstaetter, J. H., Kneussel, M., and Betz, H. (2005) Cellular localization and subcellular distribution of Unc-33-like protein 6, a brain-specific protein of the collapsin response mediator protein family that interacts with the neuronal glycine transporter 2. *J Neurochem* **94**, 307-315
 30. Horiuchi, M., El Far, O., and Betz, H. (2000) Ulip6, a novel unc-33 and dihydropyrimidinase related protein highly expressed in developing rat brain. *FEBS Lett* **480**, 283-286
 31. Warrens, A. N., Jones, M. D., and Lechler, R. I. (1997) Splicing by overlap extension by PCR using asymmetric amplification: an improved technique for the generation of hybrid proteins of immunological interest. *Gene* **186**, 29-35
 32. Bradford, M. M. (1976) A rapid and sensitive method for the quantitation of microgram quantities of protein utilizing the principle of protein-dye binding. *Anal Biochem* **72**, 248-254
 33. Torres, G. E., Yao, W. D., Mohn, A. R., Quan, H., Kim, K. M., Levey, A. I., Staudinger, J., and Caron, M. G. (2001) Functional interaction between monoamine plasma membrane transporters and the synaptic PDZ domain-containing protein PICK1. *Neuron* **30**, 121-134.
 34. Macias, M. J., Wiesner, S., and Sudol, M. (2002) WW and SH3 domains, two different scaffolds to recognize proline-rich ligands. *FEBS Lett* **513**, 30-37
 35. Li, S. S. (2005) Specificity and versatility of SH3 and other proline-recognition domains: structural basis and implications for cellular signal transduction. *Biochem J* **390**, 641-653
 36. D'Amico, A., Soragna, A., Di Cairano, E., Panzeri, N., Anzai, N., Vellea Sacchi, F., and Perego, C. (2010) The surface density of the glutamate transporter EAAC1 is controlled by interactions with PDZK1 and AP2 adaptor complexes. *Traffic* **11**, 1455-1470
 37. Dinkel, H., Michael, S., Weatheritt, R. J., Davey, N. E., Van Roey, K., Altenberg, B., Toedt, G., Uyar, B., Seiler, M., Budd, A., Jödicke, L., Dammert, M. A., Schroeter, C., Hammer, M., Schmidt, T., Jehl, P., McGuigan, C., Dymecka, M., Chica, C., Luck, K., Via, A., Chatr-aryamontri, A., Haslam, N., Grebnev, G., Edwards, R. J., Steinmetz, M. O., Meiselbach, H., Diella, F., and Gibson, T. J. (2012) ELM—the database of eukaryotic linear motifs. *Nucleic Acids Research* **40**, D242-D251
 38. Saksela, K., and Permi, P. (2012) SH3 domain ligand binding: What's the consensus and where's the specificity? *FEBS Lett* **586**, 2609-2614
 39. Sorkina, T., Miranda, M., Dionne, K. R., Hoover, B. R., Zahniser, N. R.,

- and Sorkin, A. (2006) RNA Interference Screen Reveals an Essential Role of Nedd4-2 in Dopamine Transporter Ubiquitination and Endocytosis. *J. Neurosci.* **26**, 8195-8205
40. Vaughan, R. A., and Foster, J. D. (2013) Mechanisms of dopamine transporter regulation in normal and disease states. *Trends Pharmacol Sci* **34**, 489-496
41. Shpak, M., Gentil, L. G., and Miranda, M. (2014) The origin and evolution of vertebrate glycine transporters. *J Mol Evol* **78**, 188-193
42. Miranda, M., Wu, C. C., Sorkina, T., Korstjens, D. R., and Sorkin, A. (2005) Enhanced Ubiquitylation and Accelerated Degradation of the Dopamine Transporter Mediated by Protein Kinase C. *J. Biol. Chem.* **280**, 35617-35624
43. Zeilhofer, H. U., Studler, B., Arabadzisz, D., Schweizer, C., Ahmadi, S., Layh, B., Bosl, M. R., and Fritschy, J. M. (2005) Glycinergic neurons expressing enhanced green fluorescent protein in bacterial artificial chromosome transgenic mice. *J Comp Neurol* **482**, 123-141
44. Hornbeck, P. V., Zhang, B., Murray, B., Kornhauser, J. M., Latham, V., and Skrzypek, E. (2015) PhosphoSitePlus, 2014: mutations, PTMs and recalibrations. *Nucleic Acids Res* **43**, D512-520
45. de Juan-Sanz, J., Zafra, F., Lopez-Corcuera, B., and Aragon, C. (2011) Endocytosis of the neuronal glycine transporter GLYT2: role of membrane rafts and protein kinase C-dependent ubiquitination. *Traffic* **12**, 1850-1867
46. de Juan-Sanz, J., Nunez, E., Lopez-Corcuera, B., and Aragon, C. (2013) Constitutive endocytosis and turnover of the neuronal glycine transporter GlyT2 is dependent on ubiquitination of a C-terminal lysine cluster. *PLoS One* **8**, e58863
47. Miranda, M., and Sorkin, A. (2007) Regulation of receptors and transporters by ubiquitination: new insights into surprisingly similar mechanisms. *Mol Interv* **7**, 157-167
48. Shpak, M., Gentil, L. G., and Miranda, M. (2014) The Origin and Evolution of Vertebrate Glycine Transporters. *J Mol Evol*
49. Foster, J. D., Pananusorn, B., and Vaughan, R. A. (2002) Dopamine Transporters Are Phosphorylated on N-terminal Serines in Rat Striatum. *J. Biol. Chem.* **277**, 25178-25186
50. Zita, M. M., Marchionni, I., Bottos, E., Righi, M., Del Sal, G., Cherubini, E., and Zacchi, P. (2007) Post-phosphorylation prolyl isomerisation of gephyrin represents a mechanism to modulate glycine receptors function. *EMBO J* **26**, 1761-1771
51. Specht, C. G., Grunewald, N., Pascual, O., Rostgaard, N., Schwarz, G., and Triller, A. (2011) Regulation of glycine receptor diffusion properties and gephyrin interactions by protein kinase C. *EMBO J* **30**, 3842-3853
52. Fritschy, J. M., Harvey, R. J., and Schwarz, G. (2008) Gephyrin: where do we stand, where do we go? *Trends Neurosci* **31**, 257-264
53. Tompa, P., Fuxreiter, M., Oldfield, C. J., Simon, I., Dunker, A. K., and Uversky, V. N. (2009) Close encounters of the third kind: disordered domains and the interactions of proteins. *Bioessays* **31**, 328-335
54. Paunola, E., Mattila, P. K., and Lappalainen, P. (2002) WH2 domain:

- a small, versatile adapter for actin monomers. *FEBS Lett* **513**, 92-97
55. Sudol, M., and Hunter, T. (2000) NeW wrinkles for an old domain. *Cell* **103**, 1001-1004
56. Vina-Vilaseca, A., Bender-Sigel, J., Sorkina, T., Closs, E. I., and Sorkin, A. (2011) Protein kinase C-dependent ubiquitination and clathrin-mediated endocytosis of the cationic amino acid transporter CAT-1. *J Biol Chem* **286**, 8697-8706
57. Garcia-Tardon, N., Gonzalez-Gonzalez, I. M., Martinez-Villarreal, J., Fernandez-Sanchez, E., Gimenez, C., and Zafra, F. (2012) Protein kinase C (PKC)-promoted endocytosis of glutamate transporter GLT-1 requires ubiquitin ligase Nedd4-2-dependent ubiquitination but not phosphorylation. *J Biol Chem* **287**, 19177-19187
58. Yang, B., and Kumar, S. (2010) Nedd4 and Nedd4-2: closely related ubiquitin-protein ligases with distinct physiological functions. *Cell Death Differ* **17**, 68-77
59. Lu, P. J., Zhou, X. Z., Shen, M., and Lu, K. P. (1999) Function of WW domains as phosphoserine- or phosphothreonine-binding modules. *Science* **283**, 1325-1328